

# Physical properties of apoprotein B in mixed micelles with sodium deoxycholate and in a vesicle with dimyristoyl phosphatidylcholine

Mary T. Walsh and David Atkinson

Biophysics Institute, Departments of Research Medicine and Biochemistry, Boston University School of Medicine, Housman Medical Research Center, 80 East Concord Street, Boston, MA 02118

**Abstract** Apoprotein B, the major apoprotein of normal human low density lipoprotein (LDL) was solubilized with sodium deoxycholate (NaDC). The protein was recombined with the phospholipid dimyristoyl phosphatidylcholine (DMPC) to produce a complex of DMPC-apoB (4:1 w/w). (*Biochemistry*. **22**: 3170–3178. 1983). Carboxyfluorescein and [ $^3\text{H}$ ]dextran entrapment studies show the DMPC-apoB 4:1 (w/w) complex to encapsulate an aqueous volume of  $0.17\ \mu\text{l}/\mu\text{mol}$  of DMPC. From the chemistry and morphology of the complex and the evidence that the complex possesses an encapsulated volume, the most appropriate structural model for this assembly is that of a phospholipid single bilayer vesicle into which apoB is incorporated. Differential scanning calorimetry (DSC) and circular dichroism spectroscopy (CD) were used to investigate the physical properties of apoB in the mixed micellar complex with NaDC and in the vesicular DMPC-apoB complex. CD studies of apoB in NaDC mixed micelles show that apoB exhibits a similar secondary structure as apoB of native LDL over the temperature range 5–30°C. Reversible structural changes occur between 30 and 50°C. However, above 50°C, disruption of the micellar particle and endothermic protein unfolding and denaturation occur with a  $T_{\text{max}}$  of 52°C and an enthalpy of 0.22 cal/g apoB, as shown by DSC. The DMPC-apoB complex exhibits a reversible thermal transition centered at 24°C ( $\Delta H = 3.34\ \text{Kcal/mol DMPC}$ ) which is associated with the order-disorder transition of the hydrocarbon chains of DMPC. An endothermic transition occurs over the range 53–70°C ( $\Delta H = 2.09\ \text{cal/g apoB}$ ) which, as shown by CD and turbidity study, corresponds to protein unfolding-denaturation and particle disruption. CD shows that apoB in the vesicular environment undergoes a series of conformational changes. The major alterations occur over the temperature range of the order-disorder transition of the phospholipid. Between 37–60°C, the conformation is similar to that observed in native LDL. —Walsh, M. T., and D. Atkinson. Physical properties of apoprotein B in mixed micelles with sodium deoxycholate and in a vesicle with dimyristoyl phosphatidylcholine. *J. Lipid Res.* 1986. **27**: 316–325.

**Supplementary key words** differential scanning calorimetry • circular dichroism

Numerous investigations have been conducted on the interaction of the water-soluble apoproteins of plasma

lipoproteins with phospholipid (1–5). In general, apoproteins A-I and A-II spontaneously associate with phosphatidylcholines. The composition, structure, and physical properties of the resulting complex are a function of the temperature and of the initial lipid-to-protein ratio at which the complex is formed. The C-apoproteins, C-I, C-II, and C-III, and apoprotein E also interact with phosphatidylcholines and influence the structure of the phospholipid-protein complex (3, 6).

In contrast, apoprotein B (apoB), the high molecular weight protein moiety of human low density lipoprotein (LDL) and ligand for the LDL receptor in cells of the peripheral tissue (7, 8), remains poorly characterized. Additionally, little is known concerning the details of the interaction of apoB with the lipids of LDL. This has been caused primarily by the insolubility of apoB in aqueous solutions in the absence of detergents (9–11), denaturants (12), or the lipids of native LDL.

A number of methodologies have now been reported for the solubilization of apoB from LDL and for the isolation of apoB in a lipid-free form as a mixed micellar complex with detergent (11, 13, 14). We have previously reported the solubilization of apoB using sodium deoxycholate (NaDC) and described the formation of a 4:1 (w/w) complex of apoB with the well-characterized phospholipid dimyristoyl phosphatidylcholine (DMPC) (13). In this previous study, electron microscopy was used to suggest that the complex formed with DMPC was a single bilayer vesicle of DMPC into which apoB had been incorporated.

In the work reported here we extend our previous

Abbreviations: NaDC, sodium deoxycholate; apoB, apoprotein B; LDL, low density lipoprotein; DMPC, dimyristoyl phosphatidylcholine; DSC, differential scanning calorimetry;  $\Delta H$ , experimental enthalpy;  $T_m$ , midpoint of transition;  $T_{\text{max}}$ , maximum point in transition; CD, circular dichroism; CMC, critical micellar concentration; SDS, sodium dodecyl sulfate; CF, 5(6)-carboxyfluorescein.

studies to describe the thermodynamic characterization and secondary structure of apoB as a function of temperature, in association with NaDC and in the complex with phospholipid. The results demonstrate that the thermal stability and secondary structure of apoB are dependent on the precise lipid environment and temperature. In addition, we provide evidence, using entrapment of carboxyfluorescein and [ $^3\text{H}$ ]dextran, to support a vesicular structure for the DMPC-apoB complex. These studies allow a more precise description of the molecular stoichiometry of the complex.

## MATERIALS AND METHODS

All chemicals were standard reagent grade unless otherwise indicated. 1,2-Dimyristoylphosphatidylcholine (DMPC) was purchased from Sigma (St. Louis, MO), judged to be >99% pure by thin-layer chromatography in chloroform-methanol-water 65:25:4 v/v, and used without further purification. [ $^3\text{H}$ ]Dextran was purchased from Amersham (Arlington Heights, IL). Dextran (avg mol wt 82,200 Clinical Grade) was purchased from Sigma (St. Louis, MO). Sodium (carboxyl- $^{14}\text{C}$ )deoxycholate was purchased from Amersham (Arlington Heights, IL) and judged to be 99% radiopure when chromatographed on silica gel G in chloroform-methanol-water-acetic acid 65:25:4:1 (v/v). A  $^{14}\text{C}$ -labeled DMPC stock solution in chloroform-methanol 2:1 (v/v) was made by adding L- $\alpha$ -(dipalmitoyl- $^{14}\text{C}$ )phosphatidylcholine (100 mCi/mmol) (New England Nuclear, Boston, MA) to DMPC in quantities that totalled less than 0.01 mol % of the total lipid mixture. The specific activity in disintegrations per min per mg was determined by dividing the disintegrations per min per unit volume by the dry weight (milligrams) per unit volume. The specific activity was adjusted to approximately 100,000 dpm/mg. The solution was stored at  $-20^\circ\text{C}$  under  $\text{N}_2$  in a sealed vial. 5(6)-Carboxyfluorescein was purchased from Eastman Kodak (Rochester, NY) and recrystallized from ethanol-water 1:2 prior to use.

### Lipoprotein isolation

Plasma was obtained from freshly drawn blood from normal human volunteers. Low density lipoprotein was isolated by repetitive ultracentrifugation between salt densities of 1.025 and 1.050 g/ml by the addition of solid KBr (15). Isolated LDL was washed by ultracentrifugal flotation through an overlaying solution of d 1.050 g/ml KBr, 0.02% sodium azide. All centrifugation was performed at 55,000 rpm in a Beckman L8-70 ultracentrifuge in a 70 Ti rotor for 16 hr at  $4^\circ\text{C}$ . Purity of LDL from other lipoprotein fractions was verified by agarose electrophoresis (16) by staining with Oil Red O and Coomassie Brilliant Blue.

### LDL solubilization and apoB recovery

Free sulfhydryl groups on apoB were blocked by interaction with iodoacetamide (14). LDL was dialyzed against 50 mM sodium chloride, 50 mM sodium carbonate, 0.02% sodium azide, pH 10 (standard buffer). Disruption of LDL and solubilization of its molecular constituents was achieved with sodium deoxycholate (NaDC) as previously described (13, 17). Following incubation with NaDC, fractionation was carried out by gel filtration chromatography on Sepharose CL-4B with an elution buffer containing sodium deoxycholate. ApoB was recovered in high yield in a completely delipidated form. Protein-containing column fractions were pooled and concentrated to 2 mg protein/ml by ultrafiltration and stored at  $4^\circ\text{C}$ .

### Preparation of DMPC-NaDC mixed micelles and DMPC-apoB complexes

DMPC-NaDC mixed micelles were prepared essentially as described previously (13) with the exception that DMPC of the desired mass was obtained from a radio-labeled "stock solution" as described above, dried under  $\text{N}_2$ , and desiccated in vacuo at  $4^\circ\text{C}$  overnight. Solid NaDC and 2 ml of standard buffer were then added to the dried film of lipid.

The DMPC-apoB 4:1 (w/w) complex was prepared as described previously (13). An initial lipid-to-protein ratio of 2.5:1 (w/w) was used because, according to previously published data, this ratio resulted in the highest yield of the 4:1 (w/w) DMPC-apoB complex and the least amount of uncomplexed lipid or protein.

The DMPC-apoB 4:1 (w/w) complex was isolated between the densities of 1.064 and 1.105 g/ml by density gradient ultracentrifugation (13), and dialyzed against either standard buffer (DSC samples) or 0.005 M sodium tetraborate 0.02%  $\text{NaN}_3$ , pH 10 (CD samples).

### Trapped volume determination

The presence of an intravesicular aqueous compartment in the DMPC-apoB 4:1 (w/w) complex was investigated by including [ $^3\text{H}$ ]dextran or 5(6)-carboxyfluorescein in the buffer during preparation and detergent dialysis to determine whether the complex traps either dextran or CF (nonpermeable, water-soluble molecules).

The DMPC-apoB 4:1 (w/w) complex was prepared as described previously (13), but on a smaller scale, i.e., 2 mg of NaDC-solubilized apoB was incubated with 5 mg of NaDC-solubilized DMPC for 1 hr at room temperature. NaDC was removed by dialysis as described below for each method.

**[ $^3\text{H}$ ]Dextran entrapment.** Dextran was added to the incubation mixture at a concentration of 0.1% and [ $^3\text{H}$ ]dextran to 63  $\mu\text{Ci}/2\text{ ml}$ . Dialysis was against three 200-ml changes of 50 mM sodium chloride, 50 mM

sodium carbonate, 0.02% sodium azide, 0.1% dextran, 63  $\mu\text{Ci}/200\text{ ml}$  [ $^3\text{H}$ ]dextran, pH 10, for 36 hr and then two 1-liter changes of the same buffer containing cold dextran but no [ $^3\text{H}$ ]dextran. Untrapped (free) dextran and uncomplexed protein (if any) were removed by passage of the DMPC-apoB-[ $^3\text{H}$ ]dextran mixture over a column of Sepharose CL-4B ( $1 \times 38\text{ cm}$ ) equilibrated and eluted with the same buffer as used for dialysis but without [ $^3\text{H}$ ]dextran. This column was designed to rapidly remove untrapped [ $^3\text{H}$ ]dextran from the DMPC-apoB-[ $^3\text{H}$ ]dextran incubation mixture. Column fractions were monitored for  $^{14}\text{C}$ -labeled phospholipid, [ $^3\text{H}$ ]dextran by liquid scintillation counting, and protein by the method of Lowry et al. (18) as modified by Markwell et al. (19).

**Carboxyfluorescein entrapment.** Recrystallized CF was added to the apoB-DMPC-NaDC incubation mixture to a concentration of 220 mM, a concentration at which the fluorescence of CF is self-quenched (20). The mixture was then dialyzed against three 100-ml changes of 50 mM sodium chloride, 50 mM sodium carbonate, 220 mM CF, 0.02% sodium azide, pH 10, over a period of 36 hr at  $4^\circ\text{C}$  and then two 1-liter changes of the same buffer without CF. Residual untrapped CF was removed by passage of the DMPC-apoB-CF mixture over a column of Sephadex G-50, equilibrated, and eluted with CF-free dialysis buffer. The sample size was 2 ml. Column dimensions were  $1 \times 15\text{ cm}$  and the void volume ( $V_o$ ) was 7 ml. The fraction that eluted immediately after the void volume (from 7–11 ml) contained DMPC and apoB. The DMPC-apoB 4:1 (w/w) complex was then isolated from this fraction by density gradient ultracentrifugation as previously described. The DMPC-apoB 4:1 (w/w) complex (containing CF) was dialyzed against CF-free dialysis buffer to remove KBr. Immediately prior to CF quantitation, a 1.5-ml aliquot of the complex (50  $\mu\text{mol}$  of DMPC) was removed from the dialysis bag, 50  $\mu\text{l}$  of Triton X-100 (0.3% final concentration) was added with rapid mixing, and the absorbance at 490 was monitored continuously for 2 hr. The amount of CF present in the complex was quantitated by measuring the absorbance at 490 nm in a 1-cm cell in a Perkin-Elmer Spectrophotometer (Lambda 5) (21).

### Differential scanning calorimetry

Differential scanning calorimetry (DSC) measurements were made in a Perkin-Elmer DSC-2 (Perkin-Elmer, Norwalk, CT) at heating and cooling rates of  $5^\circ\text{C}/\text{min}$  and a range of 0.2 mcal/sec, unless otherwise indicated. The DMPC-apoB 4:1 (w/w) complex was concentrated by vacuum dialysis after isolation by density gradient ultracentrifugation. NaDC-solubilized apoB was concentrated by vacuum dialysis after gel filtration chromatography. Samples were hermetically sealed in

75- $\mu\text{l}$  sample pans. The reference pan contained an equal mass of standard buffer or standard buffer plus 10 mM NaDC. Sample masses were determined either by Lowry protein (18), liquid scintillation counting, or phosphorus assay (22). Enthalpies of transition ( $\Delta H$ ) were calculated from the areas under the peaks as measured by planimetry and related to the area of the crystal-liquid melting transition of an indium standard ( $\Delta H = 6.80\text{ cal/g}$ ).

### Circular dichroism

Circular dichroic (CD) spectra of native LDL, the DMPC-apoB complex, apoB-NaDC mixed micelles, and DMPC vesicles were recorded over the temperature range  $5\text{--}70^\circ\text{C}$  on a Cary 61 spectropolarimeter calibrated with d-10-compohorsulfonic acid. The sample temperature was maintained by circulating ethylene glycol-water through the sample compartment by means of a thermostatted refrigerator-heater bath. Temperature was measured to within  $0.1^\circ\text{C}$  by means of a copper constantan thermocouple positioned in contact with the CD cell in the sample compartment. Either a 1-cm or a 1-mm quartz cell was used for measurements over the wavelength region 250–205 nm. Protein concentrations ranged from 0.03 to 0.3 mg/ml. All samples that had been prepared in standard buffer were dialyzed extensively against 0.005 M sodium tetraborate, pH 10 ( $\pm 10\text{ mM}$  NaDC as appropriate) before recording CD spectra.

All spectra reported are the average of four individual spectra on each of three to four different samples and have been corrected for baseline contributions. The possibility of a contribution to the CD spectrum from protein-free small DMPC vesicles was examined. The spectra of the protein-free vesicles at a DMPC concentration identical to that used for DMPC-apoB measurements were recorded over the wavelength region 200–250 nm at temperatures from 0 to  $60^\circ\text{C}$ . No contribution to the CD spectrum was observed at the lipid concentration used for this study over this wavelength region and temperature range. Following calculation of the molar ellipticity, the percentage of  $\alpha$ -helix was calculated and the percentage of random coil and  $\beta$ -structure was estimated according to the method of Greenfield and Fasman (23).

We have calculated the  $\alpha$ -helical content of apoB based on the molar ellipticity at 222 nm (the wavelength that corresponds to the  $n \rightarrow \pi^*$  transition of the peptide bond), utilizing the modified equation of Morrisett et al. (24). At 222 nm, the well-documented reports of differential light scattering and absorption flattening due to particle size (25, 26) are minimal. This method provides a more precise description of the  $\alpha$ -helical content of apoB, and thus the overall secondary structure of apoB, than similar calculations based on the molar ellipticity at 208 nm.

## RESULTS

### Differential scanning calorimetry and circular dichroism of mixed micelles of apoB-NaDC

The calorimetric behavior of apoB in mixed micelles with NaDC is shown in Fig. 1 and summarized in Table 1. On heating from  $-5$  to  $100^{\circ}\text{C}$ , a single endothermic transition occurs over the temperature range  $47$  to  $64^{\circ}\text{C}$  (Fig. 1A). This transition exhibits a  $T_{\text{max}}$  of  $52^{\circ}\text{C}$ , is asymmetric, has an enthalpy of  $0.22 \pm 0.02$  cal/g of apoB, and is not reversible within the time-frame of this conventional DSC experiment (Fig. 1B).

Fig. 2A–E presents characteristic CD spectra of NaDC-solubilized apoB at a number of selected temperatures. At  $6^{\circ}\text{C}$  (Fig. 2A) and  $12^{\circ}\text{C}$  (not shown), the CD spectra are both characterized by negative minima at  $220$  nm. At  $24^{\circ}\text{C}$ , the minimum of the spectrum also occurs at  $220$  nm accompanied by a small shoulder from  $209$ – $214$  nm with the molar ellipticity at  $222$  nm of  $-14.0$ .<sup>1</sup> With increasing temperature up to  $30^{\circ}\text{C}$ , the magnitude of the molar ellipticities at  $217$  and  $222$  nm decrease only slightly, indicative of only a minor alteration in the secondary structure of apoB. Above  $30^{\circ}\text{C}$ , as shown in the spectrum recorded at  $36^{\circ}\text{C}$  (Fig. 2C), the magnitude of the molar ellipticities at  $217$  and  $222$  nm are decreased slightly with respect to those observed at  $24^{\circ}\text{C}$ . These lower values at  $36^{\circ}\text{C}$  indicate that apoB has slightly less  $\alpha$ -helix, relatively little  $\beta$ -structure, and a greater amount of unordered structure as temperature is increased. At  $42^{\circ}\text{C}$  (Fig. 2D) the molar ellipticities at  $217$  and  $222$  nm are similar to those observed at  $36^{\circ}\text{C}$ , which indicates that the structural features of apoB are relatively stable between  $36$  and  $42^{\circ}\text{C}$ . Only minor variations in the overall appearance of the spectra are evident.

These alterations in secondary structure of apoB in NaDC-mixed micelles are reversible up to  $45^{\circ}\text{C}$ . Heating the sample above  $50^{\circ}\text{C}$  as shown by the spectrum recorded at  $60^{\circ}\text{C}$  (Fig. 2E) results in the loss of the secondary structure of apoB. This conversion of the ordered region of apoB to unordered or random coil coincides with the thermal event observed by DSC to occur with  $T_{\text{max}}$  of  $52^{\circ}\text{C}$ .

In an effort to characterize the molecular basis for the behavior observed by DSC and CD, a turbidity experiment was performed. The optical density, at  $280$  nm, of NaDC-solubilized apoB was measured ( $\text{OD}_{280}$  nm =  $0.311$ ,  $1$ -cm quartz cuvette, apoB =  $0.90$  mg/ml). Three identical aliquots of NaDC-solubilized apoB were placed in test tubes and heated in a water bath to  $55$ ,  $70$ , or  $100^{\circ}\text{C}$ , cooled to room temperature, and the optical density was again measured. At each of the temperatures examined, the optical density had increased to  $0.865$ . A visible aggregated flocculant material was present which

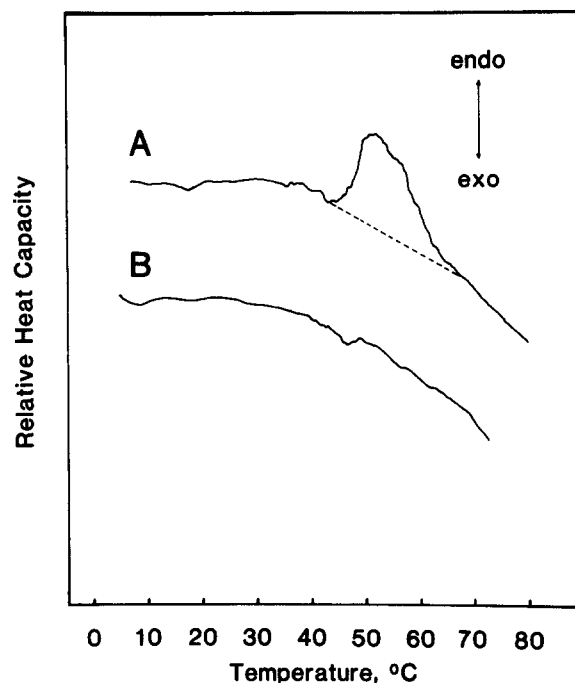


Fig. 1. Differential scanning calorimetry of apoB-NaDC mixed micelles. The mass of protein contained in the sample pan is  $1.8$  mg. A, Heating,  $-5$ – $100^{\circ}\text{C}$ ; B, final heating.

precipitated with time. Storage of the samples at room temperature overnight did not reverse this aggregation. The high concentration of NaDC ( $10$  mM), which is well above the critical micellar concentration of NaDC in this buffer, does not restore the secondary structure of apoB, as shown by the CD measurements, and apoB remains aggregated. Thus, the calorimetric transition which occurs at  $52^{\circ}\text{C}$  and is characterized by the loss of secondary structure, may be attributed to the thermal unfolding of apoB and disruption of the micellar complex.

### DMPC-apoB 4:1 (w/w) complex intravesicular aqueous compartment determination

Measurement of the amount of solute trapped by a specific amount of phospholipid has been used to provide evidence to support a vesicular structure for phospholipid systems and to provide a measure of the internal volume of a vesicle (27). The internal volume defines the size of the single bilayer vesicle.

Fig. 3 shows the gel filtration chromatographic separation of the DMPC-apoB- $^3\text{H}$ dextran incubation mixture.  $^3\text{H}$ dextran elutes as two distinct peaks. The first

<sup>1</sup>Data are expressed as the negative of the molar ellipticity  $[\theta] \times 10^{-3}$  degrees centimeters squared per decimole. The negative sign is indicative of negative absorption in the CD.



TABLE 1. Calorimetric data for the phase transitions of the apoB-NaDC mixed micellar complex and the DMPC-apoB vesicular complex

Scanning Sequence	T <sub>m</sub> , °C DMPC	T <sub>m</sub> , °C ApoB	ΔH kcal/mol DMPC	ΔH cal/g ApoB
ApoB-NaDC				
Initial heating, -5-100°C		52		0.22 ± 0.02 <sup>a</sup>
DMPC-apoB				
Initial heating, -5-50°C	24		3.34 ± 0.16 <sup>b</sup>	
Heating, -5-100°C	24	62	3.34 ± 0.16	2.09 ± 0.91 <sup>b</sup>
Final heating, -5-50°C	24		4.41 ± 0.23	

<sup>a</sup>Number of samples (n) = 9 (mean ± standard deviation).

<sup>b</sup>n = 5.

peak elutes after the void volume of the column at ~15 g of effluent and co-elutes with [<sup>14</sup>C]phospholipid and protein over two fractions. The weight ratio of DMPC to apoB in these two fractions is 4:1. The second [<sup>3</sup>H]dextran peak elutes over the range of 20 to 30 g of effluent, a position which is well separated from the phospholipid and protein-containing fractions and represents untrapped [<sup>3</sup>H]dextran. This corresponds to the same elution position as [<sup>3</sup>H]dextran applied to the same column in the absence of either DMPC or apoB.<sup>2</sup>

The trapped volume of the DMPC-apoB 4:1 (w/w) complex was calculated for the DMPC-apoB-containing column fractions using the number of moles of dextran in the fraction (specific activity of [<sup>3</sup>H]dextran = 682,582 dpm/mg), the molarity of dextran in the dialysis buffer and column buffer, and the number of moles of DMPC in the sample. These calculations gave a value for the trapped volume of the DMPC-apoB complex of 0.168 μl/μmol (± 0.013 μl/μmol, average from four samples).

A similar study was also performed utilizing the more widely used method of CF entrapment at a self-quenching concentration (20). Retention of CF at 220 mM in the complex after complete removal of untrapped CF confirms the presence of an aqueous compartment in the DMPC-apoB 4:1 (w/w) complex. This measurement yielded a trapped volume of 0.171 μl/μmol of DMPC (± 0.005 μl/μmol, average of three determinations).

#### Differential scanning calorimetry and circular dichroism of the DMPC-apoB complex

The calorimetric behavior for the DMPC-apoB complex is summarized in Fig. 4 and Table 1. On heating the DMPC-apoB complex from -5 to 50° (Fig. 4A), an endothermic transition is observed between 19 and 30°C. The transition is symmetrical with a T<sub>m</sub> at 24°C, has an enthalpy of 3.34 ± 0.16 Kcal/mol DMPC, and is completely reversible (Fig. 4B) with 3°C of undercooling.

On heating the DMPC-apoB complex to 100°C (Fig. 4C), a second endothermic transition occurs over the temperature range ~50-70°C. This transition is not

reversible over the time-frame of this experiment and is generally asymmetric. The mean onset of the transition at a heating rate of 5°C/min was at 52.3 ± 8.0°C with an end temperature of 69.3 ± 7.4°C. The peak temperature was 62.0 ± 8.0°C. As shown in Table 1, the mean enthalpy for five samples was 2.09 ± 0.91 cal/g of apoB. The temperature range of this transition is very broad. The onset and end of the transition are very gradual and therefore are difficult to determine. However, within a preparation of complex, multiple DSC samples yielded similar data.

Based on the thermal behavior of DMPC single bilayer vesicles and multilamellar liposomes (28-31), the transition observed at 24°C for the DMPC-apoB complex may be attributed to the gel to liquid crystalline transition of the hydrocarbon chains of the DMPC bilayer. This transition occurs with an enthalpy similar to that observed for small single bilayer vesicles of DMPC.

After repeated heating and cooling of the DMPC-apoB complex, over the range -5 to 100°C, the transition at 24°C sharpens and increases in enthalpy (Fig. 4D and Table 1) compared to the transition that is seen on the initial heating of the DMPC-apoB 4:1 (w/w) complex (Fig. 4A). The enthalpy approaches that observed for the corresponding transition in multilamellar liposomes of DMPC, and thus this transition represents the thermal transition of the lipid that has been liberated from the disrupted DMPC-apoB complex.

Fig. 5A-E shows characteristic CD spectra for apoB in the DMPC-apoB complex at a series of temperatures. At 6°C (Fig. 5A) the spectrum is characterized by a broad negative minimum from 220 to 225 nm and a small shoulder at ~217 nm. At this temperature the molar ellipticities at 217 and 222 are of a similar magnitude, -20.4

<sup>2</sup>Since this ratio corresponds to the ratio found in the DMPC-apoB complex, these fractions were not subjected to density gradient ultracentrifugation to purify the complex, because the complex had already been purified and eluted as two column fractions, well separated from either free phospholipid or protein.

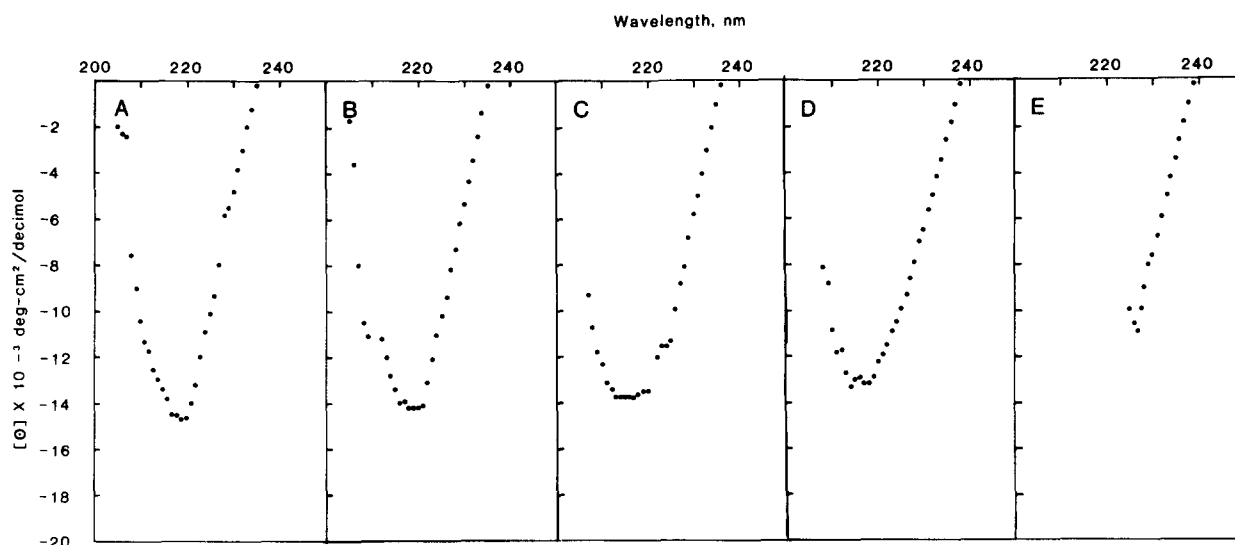


Fig. 2. Circular dichroic spectra of apoB in the mixed micellar complex with NaDC as a function of temperature. A, 6°C; B, 24°C; C, 36°C; D, 42°C; E, 60°C.

and  $-21.7$ , respectively. At  $18^\circ\text{C}$  (Fig. 5B), the spectrum exhibits a narrow minimum at  $225\text{ nm}$  accompanied by a shoulder from  $215$  to  $220\text{ nm}$ . The molar ellipticities at  $217$  and  $222$  have decreased to  $-19.1$  and  $-18.3$ , respectively, indicative of an alteration in conformation of apoB as temperature has been increased. At  $24^\circ\text{C}$  (Fig. 5C), the spectrum exhibits a minimum at  $225$ , with a slight shoulder at  $215\text{ nm}$ . The molar ellipticities at  $217$  and  $222$  ( $-16.3$  and  $-19.8$ , respectively) are indicative of a large amount of ordered structure and a greater amount of  $\alpha$ -helix than at  $18^\circ\text{C}$ . At  $42^\circ\text{C}$  (Fig. 5D) the spectrum is characterized by a broad trough from  $220$  to  $228\text{ nm}$  with a slight shoulder at  $217\text{ nm}$ . The molar ellipticities at  $217$  and  $222\text{ nm}$  decrease to  $-14.6$  and  $-18.2$ , indicating a further decrease in the helical content. These changes in spectral characteristics are reversible up to  $60^\circ\text{C}$ . As shown in the spectrum recorded at  $60^\circ\text{C}$  (Fig. 5E), the magnitude of the molar ellipticity at  $222\text{ nm}$  is  $-15.6$ , indicative of a further reduction in the  $\alpha$ -helical content of apoB in the vesicular complex with DMPC. Heating the sample above  $60^\circ\text{C}$  results in the conversion of all structured elements to random coil (not shown).

Similar to the experiment described for NaDC-solubilized apoB, a turbidity experiment was performed on the DMPC-apoB complex.  $\text{OD}_{280\text{nm}}$  of the DMPC-apoB complex was measured at room temperature (1-cm quartz cell; DMPC =  $3.3\text{ mg/ml}$ , apoB =  $0.83\text{ mg/ml}$ ;  $\text{OD}_{280} = 0.256$ ). Identical samples were then heated to  $55$ ,  $70$ , and  $100^\circ\text{C}$ , cooled to room temperature, and the optical density at  $280\text{ nm}$  was measured again. Little change in optical density was observed after heating to  $55^\circ\text{C}$  ( $\text{OD}_{280} = 0.331$ ). However, when the samples were heated to  $70^\circ\text{C}$  or  $100^\circ\text{C}$ , a large increase in turbidity was

observed ( $70^\circ\text{C}:\text{OD}_{280} = 0.534$ ;  $100^\circ\text{C}:\text{OD}_{280} = 0.932$ ). The turbidity did not reverse with storage at room temperature for  $24\text{ hr}$ . Thus, the thermal event observed by DSC that is centered at  $62^\circ\text{C}$ , and the alteration in secondary structure monitored by CD, may be attributed to the disruption of the vesicular DMPC-apoB complex and denaturation of apoB.

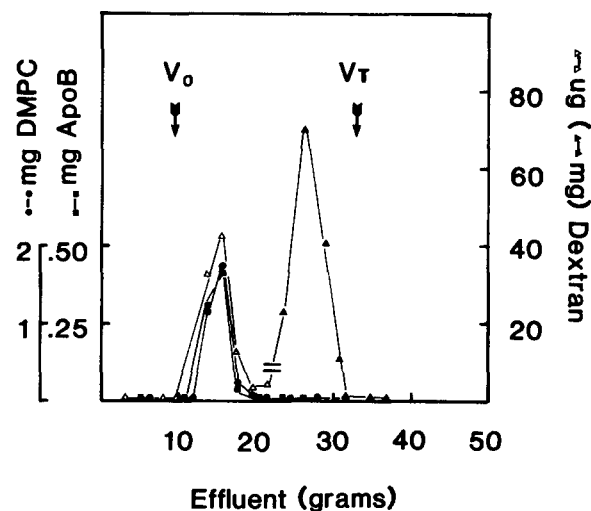
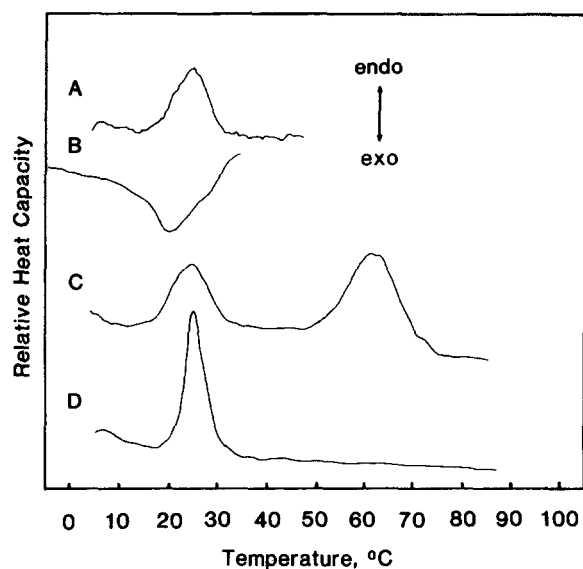


Fig. 3. Gel filtration chromatography of the DMPC-apoB- $[^3\text{H}]$ dextran incubation mixture on a  $1 \times 38\text{ cm}$  column of Sepharose Cl-4B equilibrated and eluted with  $50\text{ mM}$  sodium chloride,  $50\text{ mM}$  sodium carbonate,  $0.02\%$  sodium azide,  $0.1\%$  dextran,  $\text{pH } 10$ . Arrows mark  $V_0$  and  $V_T$ ; (●--●) phospholipid,  $\text{mg/fraction}$ ; (■--■) protein,  $\text{mg/fraction}$ ; ( $\Delta$ -- $\Delta$ )  $\mu\text{g } [^3\text{H}]$ dextran/fraction; ( $\blacktriangle$ -- $\blacktriangle$ )  $\text{mg } [^3\text{H}]$ dextran/fraction.



**Fig. 4.** Differential scanning calorimetry of DMPC-apoB 4:1 (w/w) (sample masses: 0.52 mg DMPC, 0.13 mg apoB). A, Initial heating,  $-5$ – $50^{\circ}\text{C}$ ; B, cooling,  $50$ – $-5^{\circ}\text{C}$ ; C, heating,  $-5$ – $100^{\circ}\text{C}$ ; D, final heating after several cycles over the temperature range  $-5$ – $100^{\circ}\text{C}$ .

## DISCUSSION

DSC has demonstrated that apoB in a mixed micellar complex with NaDC undergoes an endothermic transition over the temperature range  $45$ – $68^{\circ}\text{C}$  with a  $T_{\text{max}}$  of  $52^{\circ}\text{C}$  and an enthalpy of  $0.22 \pm 0.02$  cal/g apoB. This transition is associated with thermal disruption of the micellar complex and denaturation of apoB.

A more detailed analysis of the CD spectra in terms of the major components of secondary structure is shown in **Fig. 6**. Over the temperature range  $0$ – $30^{\circ}\text{C}$ , apoB in NaDC mixed micelles exhibits a similar secondary structure ( $\sim 40\%$   $\alpha$ -helix,  $\sim 20\%$   $\beta$ -sheet,  $\sim 40\%$  random coil) to apoB in native LDL. Between  $30$  and  $50^{\circ}\text{C}$ , the percentage of  $\alpha$ -helix decreases slightly; however, the percentage of  $\beta$ -sheet decreases to nearly  $0$ . The amount of unordered structure increases concomitantly to  $60\%$ . The amount of  $\alpha$  and  $\beta$  structure remains relatively stable at those values until  $50^{\circ}\text{C}$ . Up to  $50^{\circ}\text{C}$  the structural alterations are fully reversible. At this temperature the percentage of  $\alpha$ -helix decreases to  $\sim 10\%$ , the percentage of  $\beta$ -sheet increases to  $10\%$ , with the major portion of apoB ( $80\%$ ) exhibiting an unordered structure. This change is not reversible over a 24-hr time period. This loss of secondary structure occurs over the same temperature range as the endothermic transition shown by DSC (**Fig. 1**).

Prior to the characterization of the physical properties of the DMPC-apoB complex, two experiments were conducted to provide additional evidence that the appropriate structural model for this complex is a phospholipid single bilayer vesicle into which apoB is incorporated. Entrapment of either 6-carboxyfluorescein or  $[^3\text{H}]$ dextran, which are water-soluble impermeable markers, has provided firm evidence that this complex encapsulates an aqueous space and a quantitative measure for the size of this encapsulated volume. Both experiments yield a value for the entrapped volume of  $0.168$ – $0.171$   $\mu\text{l}/\mu\text{mol}$  of DMPC.

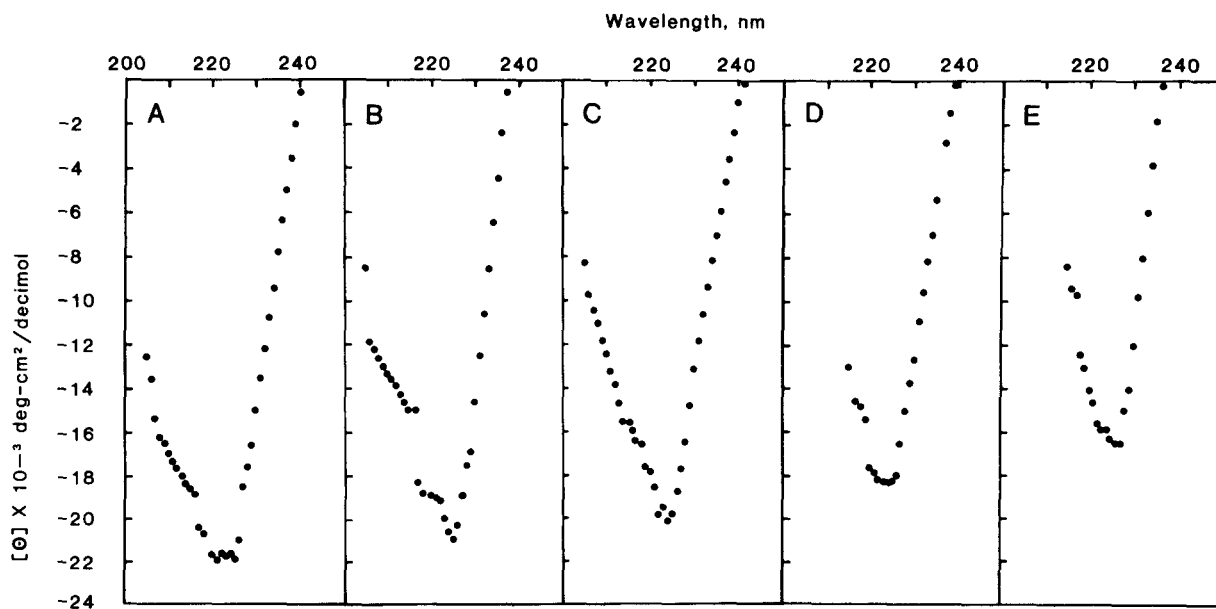


**Fig. 5.** Circular dichroic spectra of apoB in the vesicular complex with DMPC as a function of temperature. A,  $6^{\circ}\text{C}$ ; B,  $18^{\circ}\text{C}$ ; C,  $24^{\circ}\text{C}$ ; D,  $42^{\circ}\text{C}$ ; E,  $60^{\circ}\text{C}$ .

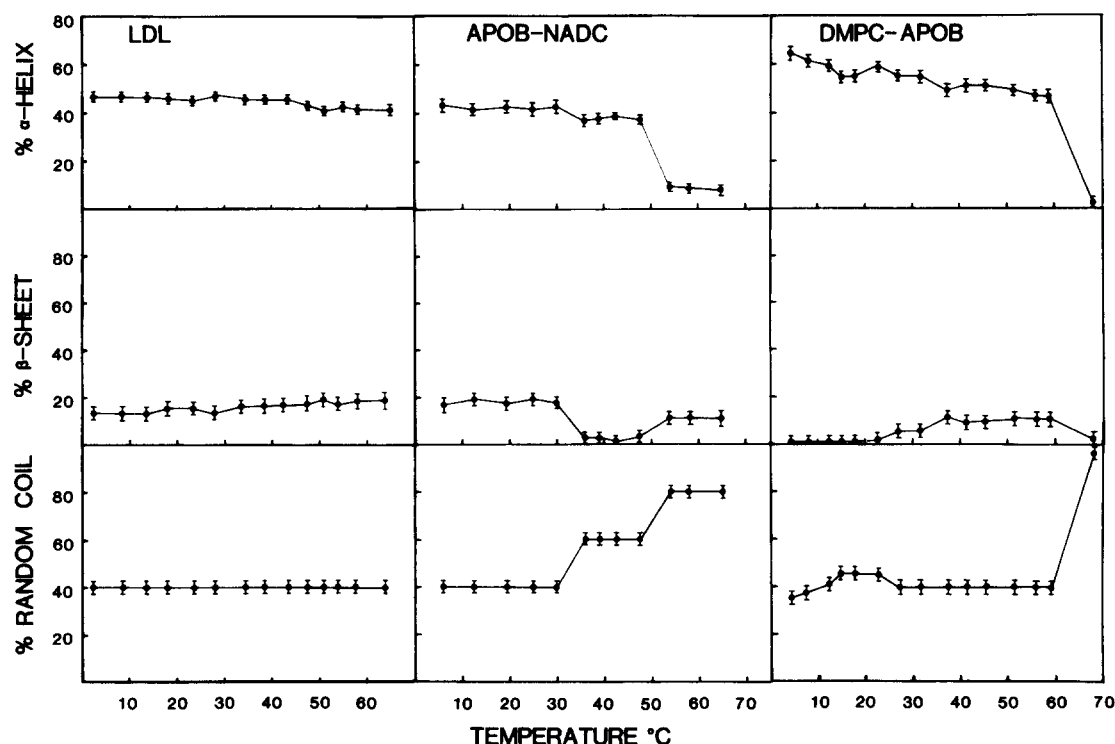


**Fig. 6.** A plot of the percentage of each secondary structural element ( $\alpha$ -helix,  $\beta$ -sheet, random coil) against temperature for apoB of LDL, NaDC-solubilized apoB, and apoB in a vesicular complex with DMPC. These data were derived from CD spectra recorded at the indicated temperatures as outlined in Methods (error bars  $\pm 1$  standard deviation of the mean derived from four or five samples). LDL exhibits its characteristic far UV-CD spectrum (13, 36–38) with a wide trough from 220 to 210 nm with molar ellipticities at 222 and 217 nm of  $-12.6$  and  $-12.8$ , respectively, indicative of a large amount of ordered structure. Only small fluctuations in secondary structural elements of apoB of native LDL are observed over the temperature range 0 to 70°C in agreement with results reported previously by Dearborn and Wetlaufer (39).

Assuming a bilayer thickness of 45 Å (32) and a DMPC cross-sectional area of 70 Å<sup>2</sup> (33), a trapped volume of 0.17  $\mu\text{l}/\mu\text{mol}$  would be calculated for a spherical, unilamellar vesicle of 200-Å diameter in the absence of protein. This value is in excellent agreement with the diameter (210 Å) for the DMPC-apoB complex determined by electron microscopy (13). Trapped volume measurements, in general (27), yield a value for the internal volume that represents an average over all vesicles in the sample population. Thus, the experimental value is heavily weighted towards vesicles of a larger size. The excellent agreement between the experimental and calculated values for the entrapment of CF and [<sup>3</sup>H]dextran indicates the uniformity in enclosed volume of all the vesicles in the sample population and thus the relative homogeneity of the DMPC-apoB 4:1 (w/w) complex.

DSC has shown the vesicular DMPC-apoB 4:1 (w/w) complex to exhibit a reversible thermal transition at a  $T_m$  of 24°C with an enthalpy of 3.34 Kcal/mol of DMPC, which may be ascribed to the gel to liquid crystalline transition of the hydrocarbon chains of the phospholipid bilayer. Comparison of the transition enthalpy for DMPC in association with apoB in the vesicular complex with that observed for DMPC sonicated unilamellar vesicles

(3.74 Kcal/mol) (30) shows that the enthalpy calculated for the protein-free vesicles and the DMPC-apoB complex are not significantly different. Thus a negligible amount of DMPC is withheld from the transition by interaction with apoB and all phospholipid molecules are available to undergo a cooperative transition.

The DMPC-apoB complex undergoes a second endothermic transition with a  $T_{max}$  of 62°C, which, as verified by a turbidity study, is associated with particle disruption. However, the  $T_m$  of the transition is at 62°C and the enthalpy associated with this transition is  $2.09 \pm 0.91$  cal/g apoB, values that are significantly greater than the enthalpy associated with the high temperature transition observed in mixed micelles of apoB with NaDC (0.22 cal/g apoB).

Fig. 6 illustrates the temperature dependence of the secondary structure of apoB in the complex with DMPC. Over the temperature range 0–15°C, the  $\alpha$ -helical content decreases from 64 to 54% and is significantly greater than that observed for apoB in LDL or in NaDC micelles (Fig. 6, left and center panels, respectively). This decrease in  $\alpha$ -helix is accompanied by a corresponding increase in unordered structure. “Random coil” structure undergoes its major change at low temperature where the DMPC bi-



layer would be in the ordered "gel" phase and reaches a constant value of ~45% prior to the onset of the phase transition at ~18°C. Over the same temperature interval there is little  $\beta$ -structure. From 18 to 32°C, which corresponds to the temperature range of the order-disorder transition of the DMPC, the amount of  $\alpha$ -helix increases slightly, accompanied by a gradual, steady increase in the amount of  $\beta$ -structure to ~10%. At 28°C, random coil decreases to 40%. From 38 to 60°C, all of the structural elements of apoB in the vesicular complex remain relatively constant ( $\alpha$  ~49.5%,  $\beta$  ~10.5%, RC ~40.0%), values which are close to those observed in native LDL (~40%  $\alpha$ -helix, ~20%  $\beta$ -sheet, ~40% random coil) over this temperature range. These changes in secondary conformation are reversible up to 59°C. Above 60°C, the  $\alpha$ -helical and  $\beta$ -sheet regions are converted to random coil and, as shown in the turbidity study, the vesicular particle is disrupted.

Thermodynamic characterization by DSC has shown that LDL undergoes two distinct thermal transitions (34). The first transition occurs reversibly over the temperature range 20–40°C in normal LDL and has been shown to be associated with an order-disorder transition of the core-located cholesteryl esters. The conformation of apoB in LDL is not altered in response to temperature over the range of 0–70°C. The secondary structural components of apoB of LDL apparently are not sensitive to this alteration of the physical state of the core lipids since the structure of apoB does not change in response to the phase transition and is invariable until ~70°C. ApoB in the mixed micellar complex with NaDC exhibits structural properties similar to apoB in its native lipid environment over the temperature range 0–30°C. From 30 to 50°C, however, reversible structural changes occur that are reflected in the  $\beta$ -sheet and random coil components. Above 52°C, all secondary structure is lost and the micellar structure is disrupted. The structural components of apoB in the vesicular environment with DMPC, however, do respond to an increase in temperature, particularly over the region of the bilayer transition. This may indicate that the conformation of apoB is determined, at least in part, by the physical state of the bilayer lipid.

A second transition in LDL occurs over the temperature range of 80–90°C and is associated with disruption of the LDL particle and protein unfolding-denaturation. Reassembled LDL complexes formed by the interaction of NaDC-solubilized apoB with preformed phospholipid-cholesteryl ester microemulsions (35) also exhibit this high temperature transition over a similar temperature range. Comparison of the behavior of apoB in mixed micelles, vesicles, and the native or reassembled LDL particle suggests that in the vesicular complex apoB has a greater thermal stability than in the mixed micellar complex with NaDC. The presence of a phospholipid bi-

layer may impart a certain amount of structural stability to apoB, since particle disruption occurs at a temperature 10°C higher in the vesicle. However, the maximum stability is provided by either the native lipid environment of LDL or phospholipid-cholesteryl ester microemulsion in the reassembled complex. In both of these systems particle disruption occurs at a high temperature. This stabilization is not due to particle size since LDL and the reassembled LDL complexes are approximately the same size as the DMPC-apoB complex. However, the presence of the cholesteryl ester core and the heterogeneity in the classes of phospholipid in the monolayer surface may be the components that ultimately stabilize the apoB molecule. ■

The authors wish to thank Dr. Donald M. Small for critically reading the manuscript, Ronald P. Corey for excellent technical assistance, and Anne M. Gibbons for expertise in preparation of the manuscript. This work was supported by United States Public Health Service grants HL-26335 and HL-07291. David Atkinson is an Established Investigator of the American Heart Association.

Manuscript received 2 July 1985.

## REFERENCES

1. Novosad, Z., R. D. Knapp, A. M. Gotto, H. J. Pownall, and J. D. Morrisett. 1976. Structure of an apolipoprotein-phospholipid complex: apoC-III induced changes in the physical properties of dimyristoylphosphatidylcholine. *Biochemistry*. **15**: 3176–3183.
2. Aune, K. C., J. G. Gallagher, A. M. Gotto, and J. D. Morrisett. 1977. Physical properties of the dimyristoylphosphatidylcholine vesicle and of complexes formed by its interaction with apolipoprotein C-III. *Biochemistry*. **16**: 2151–2156.
3. Roth, R. I., R. L. Jackson, H. J. Pownall, and A. M. Gotto. 1977. Interaction of plasma "arginine-rich" apolipoprotein with dimyristoylphosphatidylcholine. *Biochemistry*. **16**: 5030–5036.
4. Massey, J. B., A. M. Gotto, and H. J. Pownall. 1981. Thermodynamics of lipid-protein interactions of apolipoprotein A-II from human plasma high-density lipoproteins with dimyristoylphosphatidylcholine. *Biochemistry*. **20**: 1575–1584.
5. Jonas, A., S. M. Drengler, and B. W. Patterson. 1980. Two types of complexes formed by the interaction of apolipoprotein A-I with vesicles of L- $\alpha$ -dimyristoylphosphatidylcholine. *J. Biol. Chem.* **255**: 2183–2189.
6. Cardin, A. D., R. L. Jackson, and J. D. Johnson. 1982. Effects of human apolipoproteins C-I, C-II and C-III on the phase transition of sonicated vesicles of dipalmitoylphosphatidylcholine. *FEBS Lett.* **141**: 193–197.
7. Basu, S. K., R. G. W. Anderson, J. L. Goldstein, and M. S. Brown. 1977. Metabolism of cationized lipoproteins by human fibroblasts. *J. Cell. Biol.* **74**: 119–135.
8. Mahley, R. W., and T. L. Innerarity. 1978. In Sixth International Symposium on Drugs Affecting Lipid Metabolism. D. Kritchevsky, R. Paoletti, and W. L. Holmes, editors. Plenum Press, New York. 99–127.

9. Smith, R., J. R. Dawson, and C. Tanford. 1972. The size and number of polypeptide chains in human serum low density lipoprotein. *J. Biol. Chem.* **247**: 3376-3381.
10. Morrisett, J. D., R. L. Jackson, and A. M. Gotto. 1975. Lipoproteins: structure and function. *Annu. Rev. Biochem.* **44**: 183-207.
11. Steele, J. C. H., and J. A. Reynolds. 1979. Characterization of the apolipoprotein B polypeptide of human plasma low density lipoprotein in detergent and denaturant solutions. *J. Biol. Chem.* **254**: 1633-1638.
12. Steele, J. C. H., and J. A. Reynolds. 1979. Molecular weight and hydrodynamic properties of apolipoprotein B in guanidine hydrochloride and sodium dodecyl sulfate solutions. *J. Biol. Chem.* **254**: 1639-1643.
13. Walsh, M. T., and D. Atkinson. 1983. Solubilization of low-density lipoprotein with sodium deoxycholate and recombination of apoprotein B with dimyristoylphosphatidylcholine. *Biochemistry*. **22**: 3170-3178.
14. Watt, R. M., and J. A. Reynolds. 1980. Solubilization and characterization of apolipoprotein B from human serum low density lipoprotein in n-dodecyl octaethylene glycol monoether. *Biochemistry*. **19**: 1593-1598.
15. Havel, R. J., H. A. Eder, and J. H. Bragdon. 1955. Distribution and chemical composition of ultracentrifugally separated lipoproteins in human serum. *J. Clin. Invest.* **34**: 1345-1353.
16. Noble, R. P. 1968. Electrophoretic separation of plasma lipoproteins in agarose gel. *J. Lipid Res.* **9**: 693-700.
17. Helenius, A., and K. Simons. 1971. Removal of lipids from human plasma low-density lipoprotein by detergents. *Biochemistry*. **10**: 2541-2547.
18. Lowry, O. H., N. J. Rosebrough, A. L. Farr, and R. J. Randall. 1951. Protein measurement with the Folin phenol reagent. *J. Biol. Chem.* **193**: 265-275.
19. Markwell, M. A. K., S. M. Haas, L. L. Bieber, and N. E. Tolbert. 1978. A modification of the Lowry procedure to simplify protein determination in membrane and lipoprotein samples. *Anal. Biochem.* **86**: 206-210.
20. Guo, L. S. S., R. L. Hamilton, J. Goerke, J. N. Weinstein, and R. J. Havel. 1980. Interaction of unilamellar liposomes with serum lipoproteins and apolipoproteins. *J. Lipid Res.* **21**: 993-1003.
21. Roseman, M. A., B. R. Lentz, B. Sears, D. Gibbes, and T. E. Thompson. 1978. Properties of sonicated vesicles of three synthetic phospholipids. *Chem. Phys. Lipids*. **21**: 205-222.
22. McClare, C. W. F. 1971. An accurate and convenient organic phosphorus assay. *Anal. Biochem.* **39**: 527-530.
23. Greenfield, N., and G. D. Fasman. 1969. Computed circular dichroism spectra for the evaluation of protein conformation. *Biochemistry*. **8**: 4108-4116.
24. Morrisett, J. D., J. S. K. David, H. Pownall, and A. M. Gotto. 1973. Interaction of an apolipoprotein (apoLPAlanine) with phosphatidylcholine. *Biochemistry*. **12**: 1290-1299.
25. Simons, E. R. 1981. Spectroscopy in Biochemistry, Vol. I. J. E. Bell, editor. CRC Press, Inc., Boca Raton, FL. 63-153.
26. Mao, D., and B. A. Wallace. 1984. Differential light scattering and absorption flattening optical effects are minimal in the circular dichroism spectra of small unilamellar vesicles. *Biochemistry*. **23**: 2667-2673.
27. Lichtenberg, D., E. Freire, C. F. Schmidt, Y. Barenholz, P. L. Felgner, and T. E. Thompson. 1981. Effect of surface curvature on stability, thermodynamic behavior and osmotic activity of dipalmitoylphosphatidylcholine single lamellar vesicles. *Biochemistry*. **20**: 3462-3467.
28. Janiak, M. J., D. M. Small, and G. G. Shipley. 1980. Temperature and compositional dependence of the structure of hydrated dimyristoyl lecithin. *J. Biol. Chem.* **255**: 9753-9759.
29. Hinz, H.-J., and J. Sturtevant. 1972. Calorimetric studies of dilute aqueous suspensions of bilayers formed from synthetic L- $\alpha$ -lecithins. *J. Biol. Chem.* **19**: 6071-6075.
30. Ginsburg, G. S., D. M. Small, and D. Atkinson. 1982. Microemulsions of phospholipids and cholesterol esters. *J. Biol. Chem.* **257**: 8216-8227.
31. Watts, A., D. Marsh, and P. F. Knowles. 1978. Characterization of dimyristoylphosphatidylcholine vesicles and their dimensional changes through the phase transition: molecular control of membrane morphology. *Biochemistry*. **17**: 1792-1801.
32. Cornell, B. A., J. Middlehurst, and F. Separovic. 1980. The molecular packing and stability within highly curved phospholipid bilayers. *Biochim. Biophys. Acta*. **598**: 405-410.
33. Small, D. M. 1967. Phase equilibria and structure of dry and hydrated egg lecithin. *J. Lipid Res.* **8**: 551-557.
34. Deckelbaum, R. J., G. G. Shipley, and D. M. Small. 1977. Structure and interactions of lipids in human plasma low density lipoproteins. *J. Biol. Chem.* **252**: 744-754.
35. Ginsburg, G. S., M. T. Walsh, D. M. Small, and D. Atkinson. 1984. Reassembled plasma low density lipoproteins. *J. Biol. Chem.* **259**: 6667-6673.
36. Cardin, A. D., K. R. Witt, C. L. Barnhart, and R. L. Jackson. 1982. Sulfhydryl chemistry and solubility properties of human plasma apolipoprotein B. *Biochemistry*. **21**: 4503-4511.
37. Watt, R. M., and J. A. Reynolds. 1981. Interaction of apolipoprotein B with human serum low-density lipoprotein with egg yolk phosphatidylcholine. *Biochemistry*. **20**: 3897-3901.
38. Scanu, A., H. Pollard, H. Hirz, and K. Kothary. 1969. On the conformational instability of human serum low-density lipoprotein: effect of temperature. *Proc. Natl. Acad. Sci. USA*. **62**: 171-178.
39. Dearborn, D. G., and D. Wetlaufer. 1969. Reversible thermal conformation changes in human serum low-density lipoprotein. *Proc. Natl. Acad. Sci. USA*. **62**: 179-185.